

BRIEF REPORT

A quantitative method for the study of HIV-1 and *Mycobacterium tuberculosis* co-infection

Samantha Donnellan^{1,2^}, Shaun H Pennington^{1^}, Alessandra Ruggiero^{3,4^}, Carmen Martinez-Rodriguez³, Marion Pouget^{3,5}, Jordan Thomas³, Steve A Ward¹, Georgios Pollakis³, Giancarlo A Biagini^{1*} and William A Paxton^{3*}

¹Centre for Drugs and Diagnostics, Department of Tropical Disease Biology, Liverpool School of Tropical Medicine, Pembroke Place, Liverpool, L3 5QA, United Kingdom.;²School of Applied Sciences, Sighthill Campus, Edinburgh Napier University, Edinburgh, EH11 4BN, United Kingdom.; ³Department of Clinical Infection, Microbiology and Immunology, Institute of Veterinary and Ecological Sciences, University of Liverpool, 8 West Derby Street, Liverpool, L69 7BE, United Kingdom.;⁴Department of Neuroscience, Biomedicine and Movement Sciences, University of Verona, Italy;.⁵UCD Centre for Experimental Pathogen Host Research, University College Dublin, Belfield Dublin 4, Ireland.

[^]Authors equally contributing to this work.

*Giancarlo.biagini@lstm.ac.uk or WAP W.A.Paxton@liverpool.ac.uk

© The Author(s) 2022. Published by Oxford University Press on behalf of Infectious Diseases Society of America. This is an Open Access article distributed under the terms of the Creative Commons Attribution License (<https://creativecommons.org/licenses/by/4.0/>), which permits unrestricted reuse, distribution, and reproduction in any medium, provided the original work is properly cited.

M. tuberculosis and HIV-1 syndemic interactions are a major global health concern. Despite the clinical significance of co-infection, our understanding of the cellular pathophysiology and the therapeutic pharmacodynamic impact of co-infection is limited. Here, we use single-round infectious HIV-1 pseudo-typed viral-particles expressing GFP alongside *M. tuberculosis* expressing mCherry to study pathogenesis and treatment. We report that HIV-1 infection inhibited intracellular replication of *M. tuberculosis* and demonstrate the therapeutic activity of antiviral treatment (efavirenz) and antimicrobial treatment (rifampicin). The described method could be applied for detailed mechanistic studies to inform the development of novel treatment strategies.

KEYWORDS: HIV-1; *Mycobacterium tuberculosis*; TB; Co-infection; Drug screening

INTRODUCTION

Mycobacterium tuberculosis is an obligate, acid-fast, intracellular bacillus, causing the human disease tuberculosis (TB). Human Immunodeficiency Virus (HIV-1) is a lentivirus that causes acquired immune deficiency syndrome (AIDS) in humans. Both diseases are among the leading causes of death worldwide[1].

HIV-1 infected patients are up to 27-times more likely to develop active TB than non-HIV-1 infected patients and, in 2020, of the 1.3 million deaths attributed to TB, 214,000 were among HIV-1 infected individuals[2]. Infection with either pathogen can reactivate latent infection of the other, and antimicrobials targeting *M. tuberculosis* are known to interact with antivirals targeting HIV-1 [3].

Despite the clinical significance of HIV and *M. tuberculosis* co-infection, our understanding of the cellular pathophysiology and therapeutic pharmacodynamics is limited. This is in part due to the absence of quantitative methods required for study of co-infection. The development of *M. tuberculosis* and HIV-1 that carry fluorescent molecules, potentially allows for the simultaneous quantification of both pathogens using fluoresce-based modalities suitable for single-cell study and drug discovery [4,5].

We have previously used single-round infectious pseudo-typed viral particles (PVPs) to monitor antibody neutralisation of Ebola virus and for the study the glycolipid composition of pathogenic and non-pathogenic *M. tuberculosis* [6,7]. Here, we have applied similar approach to study *M. tuberculosis* and HIV-1 co-infection in THP-1 monocyte-derived macrophages. We utilise fluorometry, high-content imaging and flow cytometry to assess the impact of antiviral and antimicrobial treatment on HIV and *M. tuberculosis* co-infection.

MATERIALS AND METHODS

Cell culture

THP-1 cells were cultured in T75 flasks in RPMI-1640 supplemented with L-glutamine, NaHCO₃, 10% heat-inactivated foetal bovine serum (HI-FBS) and 100 U/mL penicillin/streptomycin, at 37 °C with 5% CO₂. For differentiation, THP-1 cells were seeded in 96-well plates (PerkinElmer®) at 1 × 10⁶ cells/well (200µL/well) in FluoroBrite DMEM supplemented with 10% HI-FBS, L-glutamine and 100ng/mL phorbol 12-myristate 13-acetate (PMA; Sigma) at 37 °C with 5% CO₂.

HEK-293T cells (ATCC: CRL1573) and TZMbl cells (NIBSC: ARP5011) were cultured in DMEM supplemented with 10% FBS and 100U/mL penicillin/streptomycin, at 37 °C with 5% CO₂.

HIV-1-PVP production

HIV-1-PVPs were produced by transfection of HEK-293T cells. One backbone plasmid expressing HIV-1 structural and polymerase proteins (pNL4-3; NIBSC: ARP12455; 2µg/10cm dish) along with a plasmid expressing either the HIV-1 BAL envelope protein (NIBSC: 140244; 2µg/10cm dish) or the vesicular stomatitis virus glycoprotein (VSV-g) envelope protein (NIBSC: 4693; 2µg/10cm dish). 48 hours post transfection, supernatant containing virus was collected, stored at -80 °C and used for downstream applications. HIV-1-PVP titres were quantified by measuring HIV-p24 protein concentration (Aalto, IRL) and virus infectivity on TZMbl cells prior to use.

M. Tuberculosis culture

H37Rv-mCherry contains an integrative plasmid (pvv16) carrying Rv2170 constitutively expressed from a HSP60 promoter (kind gift from Professor David Russell [Cornell University, USA]). Growth curves were generated according to standard procedures. Aliquots of *M. tuberculosis* H37Rv-mCherry were cultured aerobically at 37 °C in 7H9 liquid media (7H9 broth, supplemented with 0.05% [v/v] Tween-80, 0.2% [v/v] glycerol, 10% oleic acid-albumin-dextrose-catalase and 50µg/mL hygromycin). The optical density of cultures was measured at 600nm every 24 hours for 7 days. In parallel, colony forming units (CFUs) were enumerated by serial dilution and inoculation on solid media (Middlebrook 7H11 agar, supplemented with 10% oleic acid-albumin-dextrose-catalase, 0.2% [v/v] glycerol and 0.05% [v/v] Tween-80). Cultures were maintained in mid-log phase, and concentrations adjusted for infection based on growth curves.

HIV-1 and M. Tuberculosis co-infection and treatment

PVPs were added to macrophages at a concentration 30ng/well in FluoroBrite™ DMEM, supplemented with 10% heat-inactivated FBS and L-glutamine (200µL/well), as appropriate. A-PVP lacking the envelope protein (Δ Env), rendering it unable to enter target cells, was included at 30ng/well as a negative control. Concentrations were selected based on our previously published work [7]. After 24 hours, cell media were removed, and the macrophages infected with *M. tuberculosis* at a multiplicity of infection (MOI) of 1:5. The MOI was selected based on our previously published work [8]. After 24 hours the cells were washed to remove extracellular bacilli. Efavirenz in FluoroBrite™ DMEM at 10µg/mL was added to THP-1 cells 2 hours prior to infection with HIV-1 and remained in the culture media for the duration of the experiment, as appropriate. Rifampicin in FluoroBrite™ DMEM at 10µg/mL was added 24 hours after the addition of *M. tuberculosis*, as appropriate.

Confocal Laser Scanning Microscopy live imaging

Plates containing infected cells were sealed with Breath-EASIER sealing membranes (Sigma) and wrapped in parafilm. Plates were then wiped with 5% surfanios, then 70% ethanol and transferred to the confocal microscope (LSM 880; Zeiss). Z-stacks were obtained at 60× magnification.

Fluorometry

Infected plates were sealed with Breath-EASIER sealing membranes (Sigma) and wrapped in parafilm. Plates were then wiped with 5% surfanios, then 70% ethanol and transferred to the plate reader (Varioskan LUX). Fluorescence was measured at 395/409nm (excitation/emission) for GFP and 587/610nm for mCherry.

Flow cytometry

THP-1 cells were washed twice with pre-warmed PBS and then detached from the plate using ice-cold PBS and transferred to screw capped tubes. Cells were stained for viability (Pacific Blue; LifeTechnologies), washed and then incubated in 5% PFA at room temperature for 2 hours. Cells were washed once, re-suspended in ice-cold PBS and stored in the absence of light until acquisition using a FACS LSR II flow cytometer (BD Biosciences). Standard procedures were used to maintain the instrument and quality control performed daily. A compensation matrix was created, and sequential cell isolation used to identify populations using FlowJo version 10 (Treestar Inc.).

RESULTS

Co-infection of THP-1 macrophages by HIV-1 and *M. Tuberculosis*

We first confirmed that intracellular co-infection had been established by confocal microscopy (Figure 1A). For cultures infected with VSV-G HIV-1-PVP and *M. tuberculosis*, as well as for cultures infected with BAL-HIV-1-PVP and *M. tuberculosis*, co-infection was observed amongst THP-1 macrophages (Figure 1A). Visual inspection revealed that VSV-G HIV-1-PVP had a higher infectivity rate than the BAL-HIV-1-PVP (Figure 1A).

Fluorometry was utilised to study the impact of HIV-1 infection on *M. tuberculosis* growth kinetics. Over the course of 96 hours, in the absence of HIV-1-PVP, intracellular replication of *M. tuberculosis* was observed (Figure 1B). In cultures where HIV-1-VSV-G or HIV-1-BAL-PVP infection had previously been established, there was no detectable growth of *M. tuberculosis* (Figure 1B).

Single-cell assessment of *M. Tuberculosis* growth kinetics in macrophages infected with HIV-1

To improve assay resolution, we performed single-cell analysis by flow cytometry. A sequential gating strategy was used to identify THP-1 cells infected with virus and/or bacilli (Figure 2A). In cultures singularly infected with *M. tuberculosis*, approximately 31% of viable cells were infected with *M. tuberculosis* and, in cultures where HIV-1 infection had been established prior to the addition of *M. tuberculosis*, approximately 15% of viable cells were infected with *M. tuberculosis* ($p=0.0378$; Figure 2B). The addition of *M. tuberculosis* had no impact on the frequency of HIV-1 infection (Figure 2B).

Single-cell assessment of drug activity in co-infection

We next set out to demonstrate the utility of this method for the assessment of antiviral and/or antimicrobial treatment. Incubation with efavirenz was shown to block HIV-1-PVP infection (Figure 2C); approximately 5% of viable cells were singularly infected with HIV-1 in untreated control cultures and no cells were infected in cultures treated with efavirenz ($p=0.0015$); approximately 0.4% of viable cells were simultaneously infected with HIV-1 and *M. tuberculosis* in untreated control cultures and no cells were identified in cultures treated with efavirenz ($p=0.0083$; Figure 2C). Efavirenz had no impact on the frequency of cells singularly infected with *M. tuberculosis* (Figure 2C).

Incubation with rifampicin was shown to have a significant impact on the intracellular burden of *M. tuberculosis* (Figure 2C); approximately 14% of viable cells were singularly infected with *M. tuberculosis* in untreated control cultures and approximately 8% were infected in cultures treated with rifampicin ($p=0.0236$); approximately 0.4% of viable cells were simultaneously infected with HIV-1 and *M. tuberculosis* in untreated control cultures and approximately 0.07% were

identified in cultures treated with rifampicin ($p=0.0123$; Figure 2C). Rifampicin was also shown to reduce the frequency of cells singularly infected with HIV-1 – approximately 5% of viable cells were infected in untreated control cultures and approximately 0.7% of viable cells were infected in cultures treated with rifampicin ($p=0.0031$; Figure 2C).

DISCUSSION

Here, we describe a quantitative platform suitable for the study HIV-1 and *M. tuberculosis* co-infection. The described method may be applied to study disease pathogenesis and could serve to inform the development of novel treatment strategies targeting either pathogen alone, or both pathogens simultaneously.

Interestingly, and consistent with published literature [9], prior exposure to one pathogen was observed to influence the response to another subsequently encountered pathogen. Specifically, infection of macrophages with either HIV-1-VSV-G-PVP or HIV-1-BAL-PVP, prior to *M. tuberculosis* infection, resulted in sustained inhibition of intracellular growth of *M. tuberculosis*.

Pathogens can modulate cellular metabolism through direct interaction with toll-like receptors via pathogen associated molecular patterns or through indirect activation of innate immune signalling pathways. Since it is well-established that HIV-1 infection drives M1 polarisation *in vitro* [10], it is reasonable to hypothesise that pro-inflammatory polarisation may have impacted the capacity for *M. tuberculosis* to replicate intracellularly. Interestingly, since this effect was observed for both VSV-G-PVP and BAL-PVP, it can be assumed that the mechanism is independent of the viral envelope. Given that *M. tuberculosis* is also known to differently influence macrophage polarisation [11], the order in which cells encounter either HIV-1 or *M. tuberculosis* could very well influence the dynamics of disease progression and further study is warranted.

It would be an oversimplification to attempt to infer any link between the observations made here and clinical disease progression. The model presented here is unlikely to provide insight into long-term disease progression – it does, however, represent a unique platform to study the earliest stages of co-infection where HIV-1 is already established, and where *M. tuberculosis* is subsequently encountered. An appreciation of recent evidence concerning macrophage heterogeneity, in respect to both development and metabolism, indicates that the true pathophysiological representation of polarisation is far more complex [12]. Whilst simplistic definitions of M1 and M2 macrophage polarisation are useful, data presented elsewhere have demonstrated that, in reality, multiple distinct macrophage activation states exist across as spectrum [12].

Recent evidence suggests that the developmental origin of macrophages can determine their responses to infection stresses. In support, metabolic and transcriptional studies have

demonstrated that embryonically-derived alveolar macrophages and haematopoietically-derived interstitial macrophages respond differently to *M. tuberculosis* [13]. Despite this, the significance of the observations made here should not be overlooked – reduced intracellular replication of *M. tuberculosis*, is likely to prolong the time taken to sterilise the intracellular space through antimicrobial treatment and may increase risk of treatment failure.

We have demonstrated the potential utility of this platform for assessing the activity of antivirals and antimicrobials targeting HIV-1 and *M. tuberculosis*. Efavirenz is known to block the integration of viral genomic RNA and was shown to completely block HIV-1 infection. Similarly, rifampicin resulted in a reduction in the frequency of macrophages infected with *M. tuberculosis*. Interestingly, the addition of rifampicin was also shown to impact the frequency of cells identified as being singularly infected with HIV-1. Rifampicin is known to inhibit the DNA-dependent RNA polymerase of bacteria and viruses and has previously been shown to inhibit viral assembly of DNA viruses and the reverse transcriptase, RNA-directed DNA polymerase, of the Rous sarcoma virus [14,15].

It was striking that off-target effects were observed following treatment with single compounds. Given that TB and HIV treatment requires administration of multiple compounds simultaneously, we would encourage further work to understand the cellular pathophysiological impact of typical combination therapeutic strategies in the context of co-infection. Our platform affords an opportunity to assess novel combination strategies that seek to investigate potential synergistic interactions between antiviral and antimicrobial as well as host-directed immunomodulatory therapeutics. Further value could be added through inclusion of concentration-responses analysis and/or through use of primary host-cells, including monocyte derived macrophages and primary macrophages isolated from healthy volunteers HIV-infected patients. It is possible that macrophages with distinct developmental origins could show distinct phenotypes with respect to *M. tuberculosis* infectivity and intracellular growth.

FUNDING: This study was supported by the Medical Research Council (G1002586, MR/N028376/1, and MC_PC_14111 [G.A.B. and SAW]), the Wellcome Trust (105620/Z/14/Z [G.A.B. and SAW]), the UK Research and Innovation (UKRI) Strength in Places Fund (SIPF 20197 [G.A.B. and SAW]), and the European Community's Seventh Framework Programme (HEALTH-F3-2012-305578 [GP and WAP]).

TRANSPARENCY DECLARATIONS: The authors declare no conflicts of interest.

REFERENCES

1. Organization WH. Global tuberculosis report 2021. 2021. Google Scholar. **2022**; :57.
2. WHO. Global Tuberculosis Report 2014. World Health Organization. CIP data are available at <http://apps.who.int/iris>; 2014.

3. Pooranangadevi N, Padmapriyadarsini C. Treatment of Tuberculosis and the Drug Interactions Associated With HIV-TB Co-Infection Treatment. *Frontiers in Tropical Diseases*. *Frontiers*; **2022**; 0:41.
4. Aljayyousi G, Jenkins VA, Sharma R, et al. Pharmacokinetic-Pharmacodynamic modelling of intracellular Mycobacterium tuberculosis growth and kill rates is predictive of clinical treatment duration. *Sci Rep*. Nature Publishing Group; **2017**; 7(1):1–11.
5. Donnellan S, Tran L, Johnston H, McLuckie J, Stevenson K, Stone V. A rapid screening assay for identifying mycobacteria targeted nanoparticle antibiotics. *Nanotoxicology*. Taylor and Francis Ltd; **2016**; 10(6):761–769.
6. Adaken C, Scott JT, Sharma R, et al. Ebola virus antibody decay–stimulation in a high proportion of survivors. *Nature*. Nature Publishing Group; **2021**; 590(7846):468–472.
7. Pouget M, Coussens AK, Ruggiero A, et al. Generation of Liposomes to Study the Effect of Mycobacterium Tuberculosis Lipids on HIV-1 cis- and trans-Infections. *Int J Mol Sci* [Internet]. MDPI; **2021**; 22(4):1945. Available from: <https://pubmed.ncbi.nlm.nih.gov/33669411>
8. Donnellan S, Aljayyousi G, Moyo E, et al. Intracellular Pharmacodynamic Modeling Is Predictive of the Clinical Activity of Fluoroquinolones against Tuberculosis. *Antimicrob Agents Chemother* [Internet]. American Society for Microbiology; **2019**; 64(1):e00989-19. Available from: <https://pubmed.ncbi.nlm.nih.gov/31611354>
9. Bistoni F, Vecchiarelli A, Cenci E, Puccetti P, Marconi P, Cassone A. Evidence for macrophage-mediated protection against lethal *Candida albicans* infection. *Infect Immun* [Internet]. *Infect Immun*; **1986** [cited 2022 Jul 29]; 51(2):668–674. Available from: <https://pubmed.ncbi.nlm.nih.gov/3943907/>
10. Cassol E, Cassetta L, Rizzi C, Alfano M, Poli G. M1 and M2a polarization of human monocyte-derived macrophages inhibits HIV-1 replication by distinct mechanisms. *J Immunol* [Internet]. *J Immunol*; **2009** [cited 2022 Jul 29]; 182(10):6237–6246. Available from: <https://pubmed.ncbi.nlm.nih.gov/19414777/>
11. Le Y, Cao W, Zhou L, et al. Infection of Mycobacterium tuberculosis Promotes Both M1/M2 Polarization and MMP Production in Cigarette Smoke-Exposed Macrophages. *Front Immunol* [Internet]. *Front Immunol*; **2020** [cited 2022 Jul 29]; 11. Available from: <https://pubmed.ncbi.nlm.nih.gov/32973788/>
12. Xue J, Schmidt S V., Sander J, et al. Transcriptome-Based Network Analysis Reveals a Spectrum Model of Human Macrophage Activation. *Immunity*. *Immunity*; **2014**; 40(2):274–288.
13. Russell DG. Cellular Microbiology: The metabolic interface between host cell and pathogen. *Cell Microbiol*. John Wiley & Sons, Ltd; 2019. p. e13075.
14. Campbell EA, Korzheva N, Mustaev A, et al. Structural Mechanism for Rifampicin Inhibition of Bacterial RNA Polymerase. *Cell* [Internet]. **2001**; 104(6):901–912. Available from: <https://www.sciencedirect.com/science/article/pii/S0092867401002860>
15. Garriga D, Headey S, Accurso C, Gunzburg M, Scanlon M, Coulibaly F. Structural basis for the inhibition of poxvirus assembly by the antibiotic rifampicin. *Proceedings of the National Academy of Sciences* [Internet]. *Proceedings of the National Academy of Sciences*; **2018**; 115(33):8424–8429. Available from: <https://doi.org/10.1073/pnas.1810398115>

FIGURE LEGENDS

Figure 1. The impact of HIV-1 infection on the growth of intracellular *M. tuberculosis* over 96 hours in THP-1 macrophages. (A) Live-cell confocal imaging of HIV-1 and *M. tuberculosis* co-infection in THP-1 macrophage cultures singularly infected with VSV-G-HIV-1, infected simultaneously with HIV-1 VSV-G and *M. tuberculosis*, infected simultaneously with BAL-HIV-1 and *M. tuberculosis*. The green signal (green fluoresce protein) indicates host-cell infection by HIV-1. The red signal (mCherry) indicates host-cell infection by *M. tuberculosis*. All images were acquired 72 hours post infection at 63× magnification. Scale bars are representative of 50µm. Images are representative of three individual experiments. (B) The impact of HIV-1 infection on the growth of intracellular *M. tuberculosis* over 96 hours in THP-1 macrophages based on the detection of mCherry (587/610 [excitation/emission]) in arbitrary fluorescent units (AFU). Data are shown for THP-1 macrophage cultures infected with *M. tuberculosis* alone (closed circles; solid line), VSV-G-HIV-1 and *M. tuberculosis* (closed triangle; dashed and dotted line) or BAL-HIV-1 and *M. tuberculosis* (closed square; dotted line). n=3. Error bars represent the standard deviation of the mean.

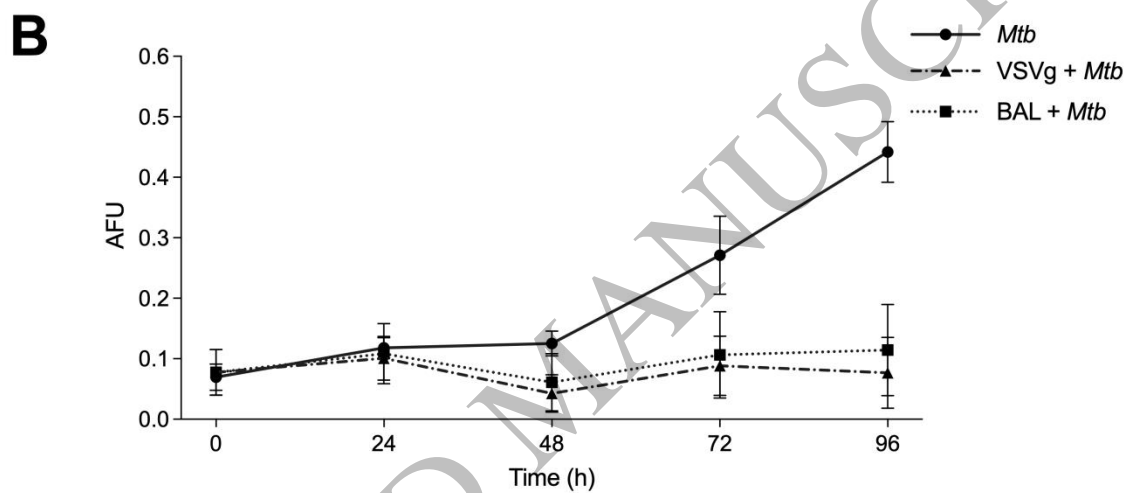
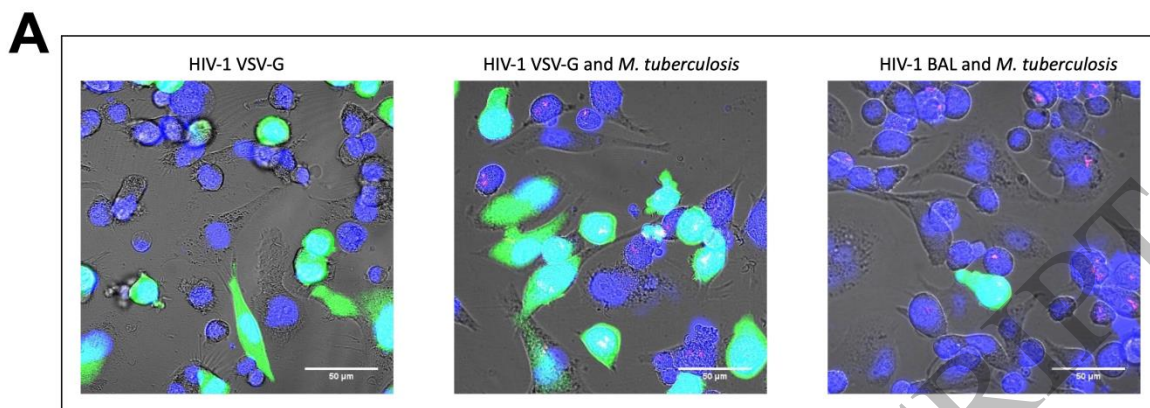


Figure 2. The impact of co-infection on the relative frequency of HIV-1 and/or *M. tuberculosis* infection in THP-1 cells. (A) Cells were identified based on their size and granularity and single cells identified based on the proportionality of area and height. Dead cells removed by staining for viability (Live/Dead) and gating on the negative population. mCherry was used to identify *M. tuberculosis* infected cells and GFP was used to identify HIV-1 infected cells. Representative dot plots are shown for THP-1 macrophages recovered from uninfected cultures (Uninfected), macrophages cultured with VSV-G HIV-1 (HIV-1), macrophages cultured with *M. tuberculosis* (*Mtb*), and macrophages cultured with both HIV and *M. tuberculosis* (HIV-1 + *Mtb*). (B) Frequency of cells infected with HIV or *M. tuberculosis* for THP-1 macrophage cultures singularly infected HIV-1 or *M. tuberculosis*, or for cultures infected simultaneously with HIV-1 VSV-G and *M. tuberculosis* is shown. N=3. Statistical comparisons were made using unpaired *t* tests. *, $p < 0.05$; NS, not significant. (C) For untreated control cultures (C) and cultures treated with efavirenz (EFV) or rifampicin (RIF), the frequency of cells singularly infected with HIV-1, singularly infected with *M. tuberculosis* or simultaneously infected with HIV-1 and *M. tuberculosis* is shown. n=3. Statistical comparisons were made using unpaired *t* tests. *, $p < 0.05$; **, $p < 0.005$; NS, not significant.

